This article has been accepted for publication in a future issue of this journal, but has not been fully edited. Content may change prior to final publication.
Citation information: DOI: 10.1109/TVT.2026.3665719, IEEE Transactions on Vehicular Technology

Waveform Design for MIMO Covert Sensing and Communications

Qiao Shi, Meiding Liu, Yi Zhou*, Zhengchun Zhou, Pingzhi Fan, *Fellow, IEEE*

***Abstract*—In this paper, we consider a multiple-input multiple-output (MIMO) integrated sensing and communications (ISAC) system, aiming at simultaneously communicating with multiple users and sensing targets that serve as adversarial observers, under multiple signal-dependent interference sources. A novel concept of covert sensing, preventing adversarial observers from detecting our sensing action or sensing intentions, is proposed, and a new metric named covert sensing distance (CSD) is established to evaluate the corresponding performance. Specifically, w e d evelop a t wo-stage s cheme. T he fi rst st age is to minimize the multi-user interference (MUI) while designing an omnidirectional transmit beampattern by constraining the CSD, to guarantee both reliable communications and covert sensing. Leveraging receiver design flexibility, t he s econd stage formulates a trade-off optimization problem by maximizing the sensing signal-to-interference-plus-noise ratio (SINR) and imposing a similarity constraint to obtain a directional receive beampattern to improve the sensing performance. To solve the formulated nonconvex problem, we propose an efficient a lternating o ptimization a lgorithm a ided b y the gradient-projection framework. Finally, the effectiveness of the proposed scheme is validated by simulation results.**

***Index Terms*—Multiple-input multiple-output, integrated sensing and communications, covert sensing distance, waveform design, multi-user interference.**

I. Introduction

Recent years have witnessed growing academic interest in integrated sensing and communications (ISAC) systems, with particular emphasis on waveform optimization techniques that enable dual-functionality operation [1]–[3]. According to different application scenarios, various ISAC waveforms are designed by optimizing both fundamental performance metrics, i.e., signal-to-interference-plus-noise ratio (SINR), integrated sidelobe level (ISL) and multi-user interference (MUI), and scenario-specific characteristics, i.e., jamming resilience, eavesdropping resistance, low probability of intercept (LPI) and covert capabilities.

Specifically, under signal-dependent modulated jamming conditions, [4] proposed a waveform optimization approach that minimizes both the jamming integrated level and ISL of the transmitted waveform, to effectively suppress the jamming. In the scenario to against eavesdroppers, the work in [5] constrained the energy transmitted to each potential eavesdropper in a multiple-input multiple-output (MIMO) ISAC system to prevent confidential information being intercepted. In the reconnaissance scenarios, [6] developed a Cramer-Rao lower bound (CRLB) detection metric through signal feature analysis to achieve LPI performance, while [7] introduced a covert communication scheme that employs symmetric Kullback-Leibler divergence as the optimization metric to prevent warden detection and enable secure communications.

Analysis reveals that the fundamental approaches in aforementioned studies primarily address two strategic paradigms: (1) direct adversarial confrontation and (2) interception prevention. From a strategic perspective, the latter strategy offers a more sustainable resolution to hostile scenarios by addressing root causes, which is also the research focus adopted in this work. To the best of our knowledge, existing ISAC research has primarily focused on LPI sensing, typically achieved through transmit power optimization [8] or sophisticated waveform design [9] to minimize exposure risks or enhance the adversary's reconnaissance challenges. However, the concept of covert sensing, which aims to conceal the sensing action or sensing intentions and actively deceive adversarial observers, remains unexplored in the literature.

To fill this gap, in this work, a novel concept of covert sensing in ISAC systems is put forward through separately designing an omnidirectional transmit beampattern[1] and a directional receive beampattern. Specifically, we consider a MIMO ISAC system that intends to simultaneously support multi-user communications and detect targets who serve as adversarial observers as well, under multiple signal-dependent interference sources. A two-stage scheme is then proposed

This work was supported in part by the National Natural Science Foundation of China under Grants U23A20274 and 62301462, in part by the Natural Science Foundation of Sichuan Province under Grant 2024NSFSC1418, in part by the China Postdoctoral Science Foundation under Grant 2023M742901, in part by UKRI Postdoc Guarantee project S-ISAC [grant number EP/Z002435/1] and EU MSCA Postdoctoral Fellowships [grant number 101154926].

Q. Shi, M. Liu and Z. Zhou are with the School of Information Science and Technology, Southwest Jiaotong University, Chengdu 611756, China (e-mail: qiaoshi@swjtu.edu.cn; lmd@my.swjtu.edu.cn; zzc@swjtu.edu.cn).

Y. Zhou is with Southwest Jiaotong University, Chengdu 610031, China, and also with Brunel University London, London, UB8 3PH (e-mail: yizhou@swjtu.edu.cn) (*Corresponding author: Yi Zhou*.)

P. Fan is with the Key Lab of Information Coding and Transmission, Southwest Jiaotong University, Chengdu 611756, China (e-mail: pzfan@swjtu.edu.cn).

[1]We aim to achieve the covert sensing through a dual-perspective framework. 1) **Power-level Undetectability**: The first objective is to avoid the sensing action being detected by the adversaries in the power domain. This is achieved by designing an omnidirectional transmit beampattern whose power is significantly lower than that of a directional beampattern in target directions. 2) **Intent-level Deception**: Recognizing that detection may sometimes be unavoidable, the second objective is to conceal the true sensing intentions, such as, detecting or tracking specific targets, which typically employs a directional beampattern, and actively mislead observers into perceiving it as general surveillance.

with the main contributions given as follows.

- A novel measurement of covert sensing distance (CSD) is proposed to indicate the maximum power difference between the designed transmit beampattern and the uniform power distributed beampattern among all directions. Based on this, an omnidirectional transmit beampattern is designed at the first stage through constraining the CSD, while minimizing the MUI to ensure reliable communications.
- To improve the intended precise sensing performance, we fully exploit the receiver's degrees of freedom at the second stage to design a directional receive beampattern through developing a trade-off optimization problem. This approach maximizes the sensing SINR while minimizing waveform similarity with the reference optimal solution derived from the preceding optimization framework. Given the nonconvex nature of the formulated problem, we develop an alternating optimization algorithm to obtain an efficient solution based on the gradient-projection framework.
- The convergence and computational complexity analyses of the proposed algorithm are discussed. Finally, simulation results validate the effectiveness of the proposed scheme, demonstrating simultaneous achievement of an omnidirectional transmit beampattern with a low CSD, a directional receive beampattern with improved SINR, and reliable communications. Furthermore, the inherent trade-offs between covert sensing, intended precise sensing, and communications are studied.

Notations: x, $\mathbf{x}$ and $\mathbf{X}$ respectively denote a scalar, vector and matrix. $\mathbb{C}^N$ and $\mathbb{C}^{N\times N}$ respectively represent the N-dimensional complex vectors and the $N\times N$-dimensional complex matrices. $\mathbf{I}_N$ indicates the N-dimensional identity matrix. $(\cdot)^T$ and $(\cdot)^H$ are the transpose and conjugate transpose operators, respectively. vec$(\cdot)$ represents the vectorisation of a matrix. $\otimes$ stands for the Kronecker product. $\mathbb{E}[\cdot]$ represents the expectation operator. $|\cdot|$ denotes the absolute value/modulus. $\|\cdot\|$ and $\|\cdot\|_F$ are the l_2 and Frobenius norms, respectively.

II. System Model

As shown in Fig. 1, we consider a MIMO ISAC system, where the ISAC base station (BS) transmits a dual-functional waveform to simultaneously communicate with K single-antenna users and sense P targets, who also serve as adversarial observers attempting to supervise operations of the ISAC BS without transmitting any signals. In addition, there are I signal-dependent interference sources aiming at disrupting the ISAC BS. The ISAC BS is equipped with a uniform linear array with N transmit antennas and M receive antennas, and the spacing between adjacent antennas is assumed to be half-wavelength.

A. Sensing Model

We assume the transmitted discrete baseband signal matrix is $\mathbf{X} = [\mathbf{x}_1, \mathbf{x}_2, \ldots, \mathbf{x}_L] \in \mathbb{C}^{N\times L}$ with $\mathbf{x}_l \in \mathbb{C}^N$ for

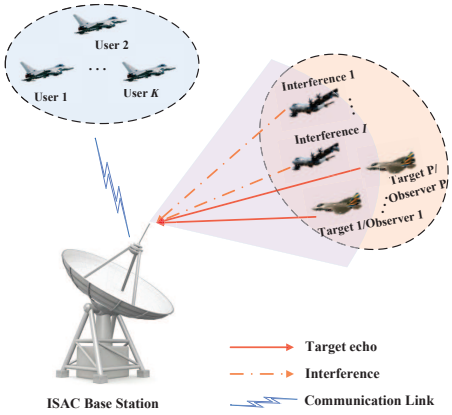

Fig. 1: A MIMO ISAC System.

$l = 1, 2, \ldots, L$ denoting the transmit vector at symbol time l and L being the length of symbol times. The targets are located at angles θ_p for $p = 1, 2, \ldots, P$, and the interference sources are located at angles ϑ_i for $i = 1, 2, \ldots, I$. Since the exact knowledge of θ_p and ϑ_i is not always available, we assume that θ_p and ϑ_i are independent uniformly distributed random variables with $\theta_p \sim U\left(\bar{\theta}_p - \delta_p/2, \bar{\theta}_p + \delta_p/2\right)$ and $\vartheta_i \sim U\left(\bar{\vartheta}_i - \bar{\delta}_i/2, \bar{\vartheta}_i + \bar{\delta}_i/2\right)$, where $\bar{\theta}_p$ and $\bar{\vartheta}_i$ are the corresponding prior means, δ_p and $\bar{\delta}_i$ denote the corresponding uncertain values, both of which can be obtained from a cognitive paradigm [10]. Then, the received signal for the ISAC BS at symbol time l can be given by

$$\mathbf{y}_l = \sum_{p=1}^{P} \alpha_p \mathbf{a}_r(\theta_p)\mathbf{a}_t^T(\theta_p)\mathbf{x}_l + \sum_{i=1}^{I} \bar{\alpha}_i \mathbf{a}_r(\vartheta_i)\mathbf{a}_t^T(\vartheta_i)\mathbf{x}_l + \mathbf{n}_l, \tag{1}$$

where α_p and $\bar{\alpha}_i$ respectively represent the responses of the pth target and the ith interference with $\mathbb{E}[|\alpha_p|^2] = \sigma_p^2$ and $\mathbb{E}[|\bar{\alpha}_i|^2] = \bar{\sigma}_i^2$, $\mathbf{a}_r(\theta) \in \mathbb{C}^M$ and $\mathbf{a}_t(\theta) \in \mathbb{C}^N$ denote the receive and transmit steering vectors, which can be respectively written as

$$\mathbf{a}_r(\theta) = [1, e^{-j\pi\sin(\theta)}, \ldots, e^{-j\pi(M-1)\sin(\theta)}]^T, \tag{2}$$

$$\mathbf{a}_t(\theta) = [1, e^{-j\pi\sin(\theta)}, \ldots, e^{-j\pi(N-1)\sin(\theta)}]^T, \tag{3}$$

and $\mathbf{n}_l$ indicates the complex white Gaussian noise vector with zero mean and covariance matrix $\tilde{\sigma}_l^2\mathbf{I}_M$.

Let $\mathbf{Y} = [\mathbf{y}_1, \mathbf{y}_2, \ldots, \mathbf{y}_L] \in \mathbb{C}^{M\times L}$, $\mathbf{Z} = [\mathbf{n}_1, \mathbf{n}_2, \ldots, \mathbf{n}_L] \in \mathbb{C}^{M\times L}$, $\mathbf{x} = \text{vec}(\mathbf{X})$, $\mathbf{y} = \text{vec}(\mathbf{Y})$ and $\mathbf{n} = \text{vec}(\mathbf{Z})$. With these definitions, the overall received signal can be written as

$$\mathbf{y} = \sum_{p=1}^{P} \alpha_p \mathbf{A}(\theta_p)\mathbf{x} + \sum_{i=1}^{I} \bar{\alpha}_i \mathbf{A}(\vartheta_i)\mathbf{x} + \mathbf{n}, \tag{4}$$

where

$$\mathbf{A}(\theta) = \mathbf{I}_L \otimes \left[\mathbf{a}_r(\theta)\mathbf{a}_t^T(\theta)\right]. \tag{5}$$

At the receiver of ISAC BS, to make full use of the degree of freedom, a receive filter $\mathbf{w}_p$ is applied to detect the pth target. As such, the filter output can be written as

$$r_p = \sum_{p=1}^{P} \alpha_p \mathbf{w}_p^H \mathbf{A}(\theta_p)\mathbf{x} + \sum_{i=1}^{I} \bar{\alpha}_i \mathbf{w}_p^H \mathbf{A}(\vartheta_i)\mathbf{x} + \mathbf{w}_p^H \mathbf{n}. \tag{6}$$

Thus, we can obtain the output SINR of the pth target as

$$\chi_p(\mathbf{x}, \mathbf{w}_p) = \frac{\sigma_p^2 |\mathbf{w}_p^H \mathbf{A}(\theta_p)\mathbf{x}|^2}{\mathbf{w}_p^H \mathbf{B}_p(\mathbf{x})\mathbf{w}_p}, \tag{7}$$

where

$$\begin{aligned}\mathbf{B}_p(\mathbf{x}) = &\sum_{j=1, j\neq p}^{P} \sigma_j^2 \mathbf{A}(\theta_j)\mathbf{x}\mathbf{x}^H \mathbf{A}^H(\theta_j) \\ &+ \sum_{i=1}^{I} \bar{\sigma}_i^2 \mathbf{A}(\vartheta_i)\mathbf{x}\mathbf{x}^H \mathbf{A}^H(\vartheta_i) + \tilde{\sigma}_l^2 \mathbf{I}_{MN}.\end{aligned} \tag{8}$$

Then, the target sensing performance can be assured by maximizing $\sum_{p=1}^{P} \chi_p(\mathbf{x}, \mathbf{w}_p)$ with jointly designing the transmitted waveform $\mathbf{x}$ and the receive filter $\mathbf{w}_p$.

In MIMO systems, the output SINR is largely determined by the beampattern. Specifically, a directional transmit beampattern is often desired to enhance the sensing performance, given by [1]

$$P_t(\theta) = \frac{1}{L} \mathbf{a}_t^H(\theta) \mathbf{X}\mathbf{X}^H \mathbf{a}_t(\theta), \tag{9}$$

which quantifies the power transmitted toward to angle θ. Moreover, for a transceiver joint design system, the output SINR can be directly characterized by the receive beampattern. It represents the signal power received from angle θ after passing through the receive filter, which is expressed as [11]

$$P_r(\theta) = \sum_{p=1}^{P} \left| \mathbf{w}_p^H \mathbf{A}(\theta)\mathbf{x} \right|^2. \tag{10}$$

Obviously, a high SINR corresponds to strong peak power in the target directions and suppressed power in interference directions, forming a directional receive beampattern.

Nevertheless, given the presence of multiple adversarial observers in the considered scenario, a directional transmit beampattern would cause them to receive strong power in target directions while detecting weak power elsewhere, particularly in interference directions, thereby revealing our target detection intent. Considering this, one novel idea is to design the transmit beampattern to distribute power uniformly across all directions (i.e., omnidirectional beampattern) while maintaining a directional receive beampattern. In this way, we can effectively prevent the sensing action from being detected or deceive adversarial observers into believing the system is conducting general surveillance rather than target detection, enabling the dual achievement of covert sensing and high-precision detection. To this end, a metric named CSD is further proposed to evaluate the covert sensing performance, which is defined as

$$\mathit{CSD} = \max_{\theta \in \Theta} \left| P_t(\theta) - P_T \right|, \tag{11}$$

where Θ denotes the set of all possible angles and P_T is the total transmit power of the ISAC system at each symbol time. This metric evaluates the similarity between the designed transmit beampattern and the ideal omnidirectional beampattern with average power P_T.

Obviously, when the transmit beampattern is omnidirectional, i.e., $P_t(\theta) = P_T, \forall \theta$, we can obtain the minimum value of CSD, i.e., $\mathit{CSD}_{\min} = 0$. Moreover, according to the expression of $\mathbf{X}$, we can rewritten (9) as

$$P_t(\theta) = \frac{1}{L} \sum_{l=1}^{L} \left| \mathbf{a}_t^H(\theta)\mathbf{x}_l \right|^2. \tag{12}$$

Thus, when $\mathbf{a}_t^H(\theta)$ is orthogonal to $\mathbf{x}_l, \forall l$, $P_t(\theta)$ reaches its minimum value with $P_t^{\min}(\theta) = 0$. When $\mathbf{a}_t^H(\theta)$ and $\mathbf{x}_l, \forall l$ are in the same direction or in opposite directions, $P_t(\theta)$ achieves its maximum value with $P_t^{\max}(\theta) = 1/L \sum_{l=1}^{L} \left| \mathbf{a}_t^H(\theta) \right|^2 |\mathbf{x}_l|^2 = NP_T$. Finally, based on the definition in (11) and the derived bounds of $P_t(\theta)$, we obtain

$$\mathit{CSD} \in [0, (N-1)P_T]. \tag{13}$$

Note that the lower the CSD, the better the covert sensing performance. As such, by enforcing the CSD to zero, we can acquire the desired transmit beampattern.

B. Communication Model

Let $\mathbf{H} \in \mathbb{C}^{K \times N}$ be the channel matrix from the ISAC BS to communication users. The received signal matrix at users can be given by

$$\mathbf{Y}^{\text{com}} = \mathbf{H}\mathbf{X} + \mathbf{Z}^{\text{com}}, \tag{14}$$

where $\mathbf{Z}^{\text{com}} = [\mathbf{z}_1, \mathbf{z}_2, \ldots, \mathbf{z}_L] \in \mathbb{C}^{K \times L}$ denotes the noise matrix with $\mathbf{z}_l \sim \mathcal{CN}(0, \check{\sigma}_z^2 \mathbf{I}_K), \forall l$.

For a given desired constellation symbol matrix $\mathbf{S} \in \mathbb{C}^{K \times L}$, the communication achievable sum rate (ASR) can be improved by minimizing the MUI energy defined as [1]

$$P_{\text{MUI}} = \|\mathbf{H}\mathbf{X} - \mathbf{S}\|_F^2. \tag{15}$$

In the following, we will formulate the specific optimization problems based on the aforementioned performance criteria.

III. Transceiver Design for Joint Sensing and Communications

In this section, a two-stage scheme is proposed for joint sensing and communications. At the first stage, we formulate an omnidirectional transmit beampattern design for covert sensing. Then, to improve the sensing performance, a directional receive beampattern is designed at the second stage.

A. Omnidirectional Beampattern Design for Covert Sensing

To achieve covert sensing, we aim to design an omnidirectional transmit beampattern so that the power is significantly lower than that of a directional beampattern in the target directions. Moreover, it can induce a deceptive perception of general surveillance, masking the true intention of detecting or tracking specific targets. Based on this idea, the following optimization problem is formulated by minimizing the MUI to maintain the communication capability, subject to the CSD constraint, i.e.,

$$\begin{aligned} &\min_{\mathbf{X}} \|\mathbf{H}\mathbf{X} - \mathbf{S}\|_F^2 \\ &s.t. \ \max_{\theta \in \Theta} |P_t(\theta) - P_T| = 0. \end{aligned} \tag{16}$$

Obviously, $\max_{\theta\in\Theta}|P_t(\theta)-P_T|=0$ indicates that $P_t(\theta)=P_T,\forall\theta\in\Theta$. According to (9), problem (16) can be equivalently transformed as

$$\begin{aligned}&\min_{\mathbf{X}}\|\mathbf{HX}-\mathbf{S}\|_F^2\\&s.t.\ \mathbf{R}_{\mathbf{X}}=\frac{P_T}{N}\mathbf{I}_N,\end{aligned}\tag{17}$$

where the left-hand-side of the constraint means the covariance matrix of $\mathbf{X}$ with $\mathbf{R}_{\mathbf{X}}=\mathbf{X}\mathbf{X}^H/L$.

Interestingly, we observe that (17) is an Orthogonal Procrustes problem and has a closed-form global solution as

$$\mathbf{X}_0=\sqrt{\frac{LP_T}{N}}\mathbf{U}\mathbf{I}_{N\times L}\mathbf{V}^{\mathrm{H}},\tag{18}$$

where $\mathbf{U}\mathbf{\Sigma}\mathbf{V}^H=\mathbf{H}^H\mathbf{S}$ denotes the singular value decomposition (SVD) of $\mathbf{H}^H\mathbf{S}$, $\mathbf{U}\in\mathbb{C}^{N\times N}$ and $\mathbf{V}\in\mathbb{C}^{L\times L}$ are unitary matrices, and $\mathbf{I}_{N\times L}$ is composed of $N\times N$ identity matrix and $N\times(L-N)$ zero matrix. Accordingly, with this transmit signal matrix $\mathbf{X}_0$, we can obtain the omnidirectional transmit beampattern and minimized MUI.

B. Directional Beampattern Design for Precise Sensing

In the above subsection, an omnidirectional transmit beampattern is designed to hide the sensing action or real target sensing intention. However, this covert sensing design may not be able to guarantee the sensing performance. Taking this into account, we introduce a similarity metric to assure the covert characteristic and communication performance, while maximizing the sensing output SINR by jointly designing the transmit waveform and receive filter to obtain a directional receive beampattern. Finally, with constant modulus constraint considered, we construct a trade-off optimization problem as

$$\begin{aligned}\min_{\mathbf{x},\{\mathbf{w}_p\}_{p=1}^P}\ &\rho\|\mathbf{x}-\mathbf{x}_0\|^2+\frac{1-\rho}{\sum_{p=1}^P\chi_p(\mathbf{x},\mathbf{w}_p)}\\s.t.\quad&|x_n|=\sqrt{\frac{P_T}{N}},\forall n,\end{aligned}\tag{19}$$

where ρ indicates the weight factor applied to balance the detection capability, covert sensing and communication performance, $\mathbf{x}_0=\mathrm{vec}(\mathbf{X}_0)$, $\sum_{p=1}^P\chi_p(\mathbf{x},\mathbf{w}_p)$ is the sum of sensing output SINR of P targets, and x_n denotes the nth entry of waveform $\mathbf{x}$. Obviously, a larger ρ represents that more resources are allocated to optimize the CSD and communication performance, resulting in the degradation of sensing SINR performance, and vice versa.

As can be seen, (19) is a nonconvex optimization problem involving two coupled variables, requiring specialized solution approaches. Therefore, we propose an alternating optimization algorithm to divide the original problem into two subproblems, and solve them respectively. The specific procedures are given as follows.

1) Solving filters $\{\mathbf{w}_p\}_{p=1}^P$: For solving the receive filter $\mathbf{w}_p$, the transmit waveform $\mathbf{x}$ is considered as a constant and the constant modulus constraint is ignored as it is independent of $\mathbf{w}_p$. Then, the optimization problem can be simplified as

$$\max_{\{\mathbf{w}_p\}_{p=1}^P}\ \chi_p\left(\mathbf{x},\mathbf{w}_p\right),\tag{20}$$

which can be further written as

$$\begin{aligned}\min_{\{\mathbf{w}_p\}_{p=1}^P}\ &\mathbf{w}_p^H\mathbf{B}_p(\mathbf{x})\mathbf{w}_p\\s.t.\ \ &\mathbf{w}_p^{\mathrm{H}}\mathbf{A}(\theta_p)\mathbf{x}=1.\end{aligned}\tag{21}$$

Then, the closed-form solution can be obtained by [12]

$$\mathbf{w}_p=\frac{\mathbf{B}_p^{-1}(\mathbf{x})\mathbf{A}(\theta_p)\mathbf{x}}{\mathbf{x}^H\mathbf{A}^H(\theta_p)\mathbf{B}_p^{-1}(\mathbf{x})\mathbf{A}(\theta_p)\mathbf{x}}.\tag{22}$$

2) Solving transmit waveform $\mathbf{x}$*:* Similarly, by fixing the receive filters $\{\mathbf{w}_p\}_{p=1}^P$, the optimization problem to solve $\mathbf{x}$ is written as

$$\begin{aligned}\min_{\mathbf{x}}\ &\rho\|\mathbf{x}-\mathbf{x}_0\|^2+\frac{1-\rho}{\sum_{p=1}^P\chi_p(\mathbf{x},\mathbf{w}_p)}\\s.t.\ &|x_n|=\sqrt{\frac{P_T}{N}},\forall n.\end{aligned}\tag{23}$$

To solve (23), we adopt the gradient-projection (GP) framework [13]. In specific, we let

$$g(\mathbf{x},\mathbf{w}_p)=\rho\|\mathbf{x}-\mathbf{x}_0\|^2+\frac{1-\rho}{\sum_{p=1}^P\chi_p(\mathbf{x},\mathbf{w}_p)},\tag{24}$$

$$\mathbf{d}=\mathbf{x}-\alpha\nabla_{\mathbf{x}}g(\mathbf{x},\mathbf{w}_p),\tag{25}$$

where α denotes the step-size parameter,

$$\nabla_{\mathbf{x}}g(\mathbf{x},\mathbf{w}_p)=2\rho(\mathbf{x}-\mathbf{x}_0)-(1-\rho)\frac{\sum_{p=1}^P\nabla_{\mathbf{x}}\chi_p(\mathbf{x},\mathbf{w}_p)}{\left(\sum_{p=1}^P\chi_p(\mathbf{x},\mathbf{w}_p)\right)^2},\tag{26}$$

$$\nabla_{\mathbf{x}}\chi_p(\mathbf{x},\mathbf{w}_p)=\frac{2\mathbf{G}_1\mathbf{x}b-2\mathbf{x}^H\mathbf{G}_1\mathbf{x}\mathbf{G}_2\mathbf{x}}{|b|^2},\tag{27}$$

$$b=\mathbf{x}^H\mathbf{G}_2\mathbf{x}+\tilde{\sigma}_l^2\mathbf{w}_p^H\mathbf{w}_p,\tag{28}$$

$$\mathbf{G}_1=\sigma_p^2\mathbf{A}^H(\theta_p)\mathbf{w}_p\mathbf{w}_p^H\mathbf{A}(\theta_p),\tag{29}$$

$$\mathbf{G}_2=\sum_{j=1,j\neq p}^P\sigma_j^2\mathbf{A}^H(\theta_j)\mathbf{w}_p\mathbf{w}_p^H\mathbf{A}(\theta_j)+\sum_{i=1}^I\bar{\sigma}_i^2\mathbf{A}^H(\vartheta_i)\mathbf{w}_p\mathbf{w}_p^H\mathbf{A}(\vartheta_i).\tag{30}$$

Then, a closed-form solution of $\mathbf{x}$ can be given as

$$x_n=\begin{cases}\sqrt{\dfrac{P_T}{N}}, & d_n=0\\ \sqrt{\dfrac{P_T}{N}}\dfrac{d_n}{|d_n|}, & d_n\neq 0,\end{cases}\tag{31}$$

where d_n represents the nth entry of $\mathbf{d}$. Therefore, by alternately solving $\mathbf{w}_p$ and $\mathbf{x}$ until convergence, the final solution to the optimization problem (19) can be obtained.

It is worth noting that at each iteration, the $\mathbf{w}_p$-subproblem (20) is solved in closed form, whereas the $\mathbf{x}$-subproblem (23) is updated through a GP step based on a locally tight surrogate that satisfies the majorization and first-order consistency properties. These properties ensure a monotonic decrease of the objective, which is lower bounded and thus convergent. Following the well-established convergence arguments in [11], any accumulation point of the iterates satisfies the first-order optimality conditions with respect to both block variables.

Therefore, the proposed algorithm converges to a stationary point of problem (19).

The overall complexity is discussed as follows. The proposed algorithm consists of two optimization stages. Problem (16) is solved once with a computational complexity of $O(NKL + NL^2)$. Subsequently, problem (19) is solved via an alternating optimization procedure, where $\mathbf{w}_p$ is updated in closed form and $\mathbf{x}$ is updated using a GP step. The per-iteration complexity of problem (19) is $O\left(PM^3L^3 + P\left(P+I\right)MNL^2\right)$. With η iterations, the total computational complexity is therefore $O\left(NKL + \eta\left(PM^3L^3 + P\left(P+I\right)MNL^2\right)\right)$.

IV. Simulation Results

In this section, we aim to verify the sensing and communication performance through simulation experiments. The numbers of transmit and receive antennas are set to $N = M = 16$, unless otherwise stated. The number of communication users is set to $K = 4$. There are two targets located at $\bar{\theta}_1 = -40^\circ$ and $\bar{\theta}_2 = 15^\circ$, each with a power of $\sigma_1^2 = \sigma_2^2 = 10\,\text{dB}$. Two interference sources are separately located at $\bar{\vartheta}_1 = -10^\circ$ and $\bar{\vartheta}_2 = 40^\circ$ with power $\bar{\sigma}_1^2 = \bar{\sigma}_2^2 = 30\,\text{dB}$. The noise variance at the ISAC BS is set to $\tilde{\sigma}_l^2 = 0\,\text{dB}$. The total symbol times is $L = 20$ and the total transmit power is set to $P_T = 1\,\text{W}$. The constellation is obtained by the unit power Quadrature Phase Shift Keying (QPSK) alphabet and the channel coefficients are subject to $\mathcal{CN}(0,1)$. The results are averaged over 100 Monte Carlo simulations.

Fig. 2 shows the convergence curves with different values of the step-size parameter α. The iteration termination condition is set as $\left|g\left(\mathbf{x}^{(t+1)}, \mathbf{w}_p^{(t+1)}\right) - g(\mathbf{x}^{(t)}, \mathbf{w}_p^{(t)})\right| \leq 10^{-3}$. As can be seen, the proposed algorithm is monotonically decreasing and is guaranteed to converge to a fixed value. To facilitate the following simulations, the α is set to 0.1.

Fig. 3 plots the proposed transmit beampattern ('Omni'), the proposed receive beampattern ('Directional') and the optimal beampattern ('Omni-opt') obtained by solving problem (16). As can be seen, the Omni-opt solution generates a perfectly omnidirectional transmit beampattern, while the proposed Omni design achieves near-ideal approximation with larger value of the weight factor ρ. This isotropic power distribution

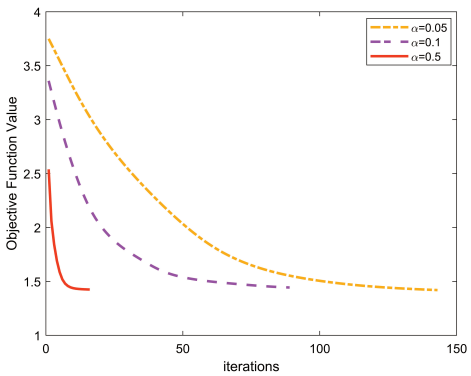

Fig. 2: Convergence curves with a weight factor $\rho = 0.5$.

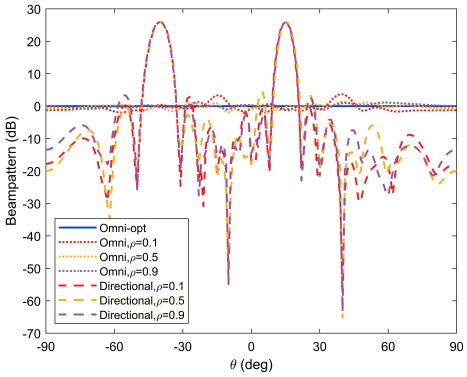

Fig. 3: Beampatterns with different weight factors ρ.

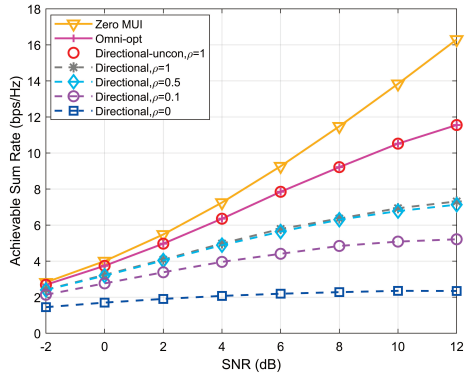

Fig. 4: ASR with different weight factors ρ.

effectively conceals directional transmission characteristics, preventing adversarial detection of our sensing action or true intentions. In addition, by observing the proposed directional receive beampattern, we see that the formulated beampattern demonstrates precise energy focusing in the target directions with simultaneous interference suppression, thus improving the precise target sensing capability. In summary, by separately designing the transmit and receive beampatterns, we successfully accomplish both covert sensing and intended precise sensing.

Next, the communication performance in terms of the ASR with respect to signal-to-noise ratio (SNR) is displayed in Fig. 4, where the SNR is defined as $P_T/\tilde{\sigma}_z^2$. It can be seen that the Omni-opt always outperforms the proposed design and approaches the theoretical upper bound established by the Zero MUI reference case. This phenomenon results from competing optimization objectives in (19), where substantial resources must simultaneously optimize sensing criterion and satisfy strict constant modulus properties ('Directional-uncon' indicates a configuration without the constant modulus constraint, displaying the same performance with Omni-opt), leaving limited capacity for communication ASR enhancement. By observing curves with different values of weight factor ρ, it is obvious that the case of $\rho = 0$ (sensing-only optimization) leads to the poorest communication ASR, while increasing ρ displays consistent communication performance improvement.

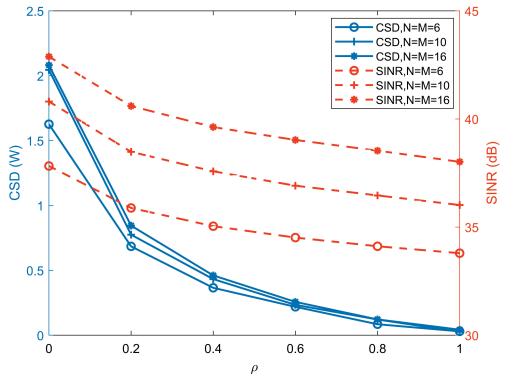

Fig. 5: CSD and SINR curves with the weight factor ρ.

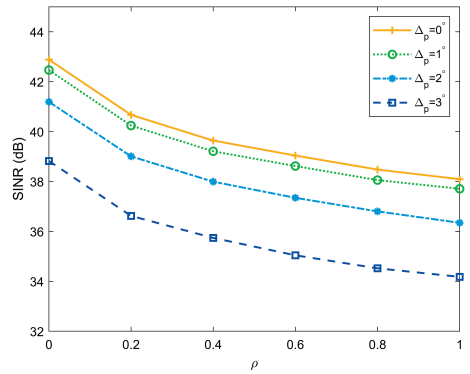

Fig. 6: SINR curves with target angle estimation errors.

Then, the tripartite performance trade-offs are systematically discussed. As shown in Fig. 5, we plot the CSD (blue) and sensing output SINR (orange) curves with respect to the weight factor ρ. Results reveal that increasing the number of antennas enhances SINR by offering more design flexibility, yet simultaneously leads to a degradation in CSD performance. Combining with Fig. 4, we see that higher ρ values yield lower CSD and SINR but increased ASR, reflecting improved covert sensing and communication capabilities at the cost of reduced sensing performance. Moreover, when $\rho = 1$, the CSD almost attains its lower bound ($CSD = 0$), indicating superior covert sensing performance. However, in practical scenarios, perfect covert sensing performance is not always required. Therefore, we can appropriately reduce ρ to enhance the intended precise sensing performance while maintaining satisfactory communication performance. In summary, by suitably adjusting ρ referring to Fig. 5, we can achieve trade-offs between covert sensing, intended precise sensing and communication performance.

Finally, we have also analyzed the impact of target angle estimation errors $\Delta_p = \left|\bar{\theta}_p - \theta_p\right|$ for $p = 1, 2$ on sensing SINR. As shown in Fig. 6, the sensing SINR decreases as the weight factor ρ increases, and also degrades with larger angle estimation errors. However, even with $\rho = 1$ and angle estimation error $\Delta_p = 3^\circ$, the output SINR achieves 34.2 dB, which generally meets typical detection requirements and confirms the effectiveness of the proposed design.

V. Conclusion

In this paper, a joint covert sensing and communication scheme has been proposed in MIMO ISAC systems. We have first proposed a covert sensing metric named CSD and subsequently developed an omnidirectional transmit beampattern design by minimizing the MUI and constraining the CSD. Then, to improve the intended precise sensing capability, we have maximized the sensing SINR while introducing the similarity metric to obtain a directional receive beampattern. Finally, simulation results indicate that our proposed scheme can simultaneously realize covert sensing, intended precise sensing, and reliable communications. Promising future directions include the joint optimization of covert communication and covert sensing, along with scenarios involving distributed targets and mobile interference sources, as well as the use of alternative detection metric, such as mutual information and the Kullback-Leibler divergence.

References

[1] F. Liu, L. Zhou, C. Masouros, A. Li, W. Luo and A. Petropulu, "Toward Dual-functional Radar-Communication Systems: Optimal Waveform Design," *IEEE Trans. Signal Process.*, vol. 66, no. 16, pp. 4264-4279, Aug. 2018.

[2] T. -X. Zheng, X. Chen, L. Lan, Y. Ju, X. Hu, R. Liu, D. Ng and T. Cui, "Reconfigurable Intelligent Surface-Aided Secure Integrated Radar and Communication Systems," *IEEE Trans. Wireless Commun.*, vol. 24, no. 3, pp. 1934-1948, Mar. 2025.

[3] P. Liu, Z. Fei, X. Wang, Y. Zhou, Y. Zhang and F. Liu, "Joint Beamforming and Offloading Design for Integrated Sensing, Communication, and Computation System," *IEEE Trans. Veh. Technol.*, vol. 74, no. 9, pp. 14933-14937, Sept. 2025.

[4] Y. Zhou, Q. Shi, Z. Zhou, Z. Liu and P. Fan, "Waveform and Filter Design for Integrated Sensing and Communication Against Signal-dependent Modulated Jamming," *IEEE Trans. Veh. Technol.*, vol. 74, no. 8, pp. 12480-12495, Aug. 2025.

[5] D. Li, B. Tang and L. Xue, "Waveform Design for MIMO DFRC Systems: Finer Sensing and Safer Communications," *IEEE Trans. Signal Process.*, vol. 72, pp. 4509-4524, 2024.

[6] X. Liu, Y. Yuan, T. Zhang, G. Cui and W. P. Tay, "Integrated Transmit Waveform and RIS Phase Shift Design for LPI Detection and Communication," *IEEE Trans. Wireless Commun.*, vol. 23, no. 6, pp. 5663-5679, Jun. 2024.

[7] J. Hu, Q. Lin, S. Yan, X. Zhou, Y. Chen and F. Shu, "Covert Transmission via Integrated Sensing and Communication Systems," *IEEE Trans. Veh. Technol.*, vol. 73, no. 3, pp. 4441-4446, Mar. 2024.

[8] C. Shi, X. Zhang, Z. Shi, J. Zhou and J. Yan, "Joint Detection Threshold Optimization and Multidimensional Resource Allocation Scheme for Multitarget Tracking in Radar Networks Based on Low Probability of Intercept," *IEEE Trans. Aerosp. Electron. Syst.*, vol. 61, no. 2, pp. 1433-1453, Apr. 2025.

[9] Q. Shi, Y. Wang, Z. Zhou, G. Cui and P. Fan, "Low Probability of Intercept Signal Design for MIMO Integrated Sensing and Communication Systems," *IEEE Trans. Commun.*, vol. 73, no. 9, pp. 8155-8165, Sept. 2025.

[10] G. Cui, X. Yu, V. Carotenuto and L. Kong, "Space-Time Transmit Code and Receive Filter Design for Colocated MIMO Radar," *IEEE Trans. Signal Process.*, vol. 65, no. 5, pp. 1116-1129, Mar. 2017.

[11] C. G. Tsinos, A. Arora, S. Chatzinotas and B. Ottersten, "Joint Transmit Waveform and Receive Filter Design for Dual-Function Radar-Communication Systems," *IEEE J. Sel. Topics Signal Process.*, vol. 15, no. 6, pp. 1378-1392, Nov. 2021.

[12] G. Cui, H. Li and M. Rangaswamy, "MIMO Radar Waveform Design With Constant Modulus and Similarity Constraints," *IEEE Trans. Signal Process.*, vol. 62, no. 2, pp. 343-353, Jan. 2014.

[13] D. P. Bertsekas, "Nonlinear programming," *J. Oper. Res. Soc.*, vol. 48, no. 3, pp. 334-334, 1999.